Roll-able Multisegment Dielectric Elastomer Minimum Energy Structures for a Deployable Microsatellite Gripper

Oluwaseun A. Araromi, Irina Gavrilovich, Jun Shintake, Samuel Rosset, Muriel Richard, Volker Gass, Herbert R. Shea

http://dx.doi.org/10.1109/TMECH.2014.2329367

Roll-able Multisegment Dielectric Elastomer Minimum Energy Structures for a Deployable Microsatellite Gripper

Oluwaseun A. Araromi, Irina Gavrilovich, Jun Shintake, Samuel Rosset, Muriel Richard, Volker Gass, Herbert R. Shea (*IEEE* Senior Member)

Abstract—**Debris in space present an ever-increasing problem for spacecraft in Earth orbit. As a step in the mitigation of this issue, the CleanSpace One (CSO) microsatellite has been proposed. Its mission is to perform active debris removal of a decommissioned nanosatellite (the CubeSat SwissCube). An important aspect of this project is the development of the gripper system that will entrap the capture target. We present the development of roll-able dielectric elastomer minimum energy structures (DEMES) as the main component of CSO's deployable gripper. DEMES consist of a prestretched dielectric elastomer actuator membrane bonded to a flexible frame. The actuator finds equilibrium in bending when the prestretch is released and the bending angle can be changed by the application of a voltage bias. The inherent flexibility and lightweight nature of the DEMES enables the gripper to be stored in a rolled-up state prior to deployment. We fabricated proof of concept actuators of three different geometries using a robust and repeatable fabrication methodology. The resulting actuators were mechanically resilient to external deformation, and display conformability to objects of varying shapes and sizes. Actuator mass is less than 0.65 g and all the actuators presented survived the rolling-up and subsequent deployment process. Our devices demonstrate a maximum change of bending angle of more than 60 degrees and a maximum gripping (reaction) force of 2.2 mN for a single actuator.**

Index Terms— **Active debris removal (ADR), artificial muscles, deployable mechanism, dielectric elastomer actuator (DEA), space debris.**

I. INTRODUCTION

The field of space exploration is rapidly expanding with over one hundred new satellites placed into orbit every

O. Araromi, J. Shintake, S. Rosset and H. Shea are with the Microsystems for Space Technologies Laboratory, École Polytechnique Fédérale de Lausanne (EPFL), Rue de la Maladière 71B, Neuchatel 2000, Switzerland (email: seun.araromi@epfl.ch; jun.shintake@epfl.ch; samuel.rosset@epfl.ch; herbert.shea@epfl.ch).

M. Richard and V. Gass are with the Swiss Space Center, École Polytechnique Fédérale de Lausanne (EPFL), Lausanne, Switzerland (email: muriel.richard@epfl.ch; volker.gass@epfl.ch). Irina Gavrilovich was with the Swiss Space Center, École Polytechnique Fédérale de Lausanne (EPFL), Lausanne, Switzerland (email: irina.gavrilovich@lirmm.fr).
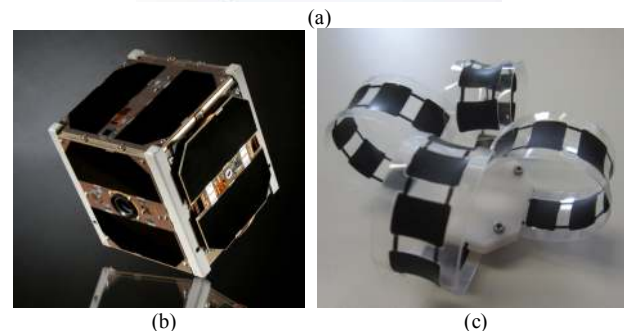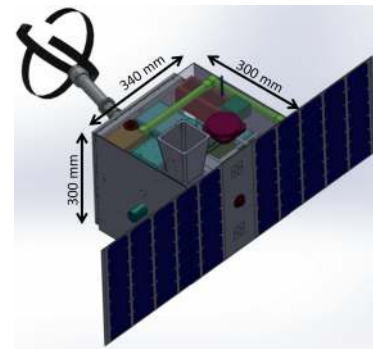

Fig. 1. (a) Proposed design for the CleanSpace One (CSO) satellite with conceptualized gripper, planned for launch in 2018 [1]. (b) Photo of SwissCube, the capture target for CSO's first mission, a 100 mm × 100 mm × 100 mm CubeSat launched in September 2009 [2]. (c) Model of proposed deployable, multisegment dielectric elastomer minimum energy structure gripper for CSO.

year. With each launch space debris is produced in the form of remnants from the launch (e.g. rocket bodies), or when the satellites themselves reach the end of their useful life [1], [3]. Such debris present an ever-increasing risk to satellites and other spacecraft, as highlighted in 2009 by the high-velocity collision between the then operational Iridium 33 and the inactive Kosmos 2251 satellites [3].

A solution has been proposed for tackling this problem in the shape of CleanSpace One (CSO) [4] (Fig. 1(a)), a low cost microsatellite (~30-40 kg) which aims to perform active debris removal (ADR). CSO is expected to launch in 2018 and its primary mission is to rendezvous and entrap a decommissioned nanosatellite currently in orbit at 750 km altitude (Fig. 1(b)), then deorbit the CubeSat. Though ADR for CubeSats is not the ultimate goal for this technology, this
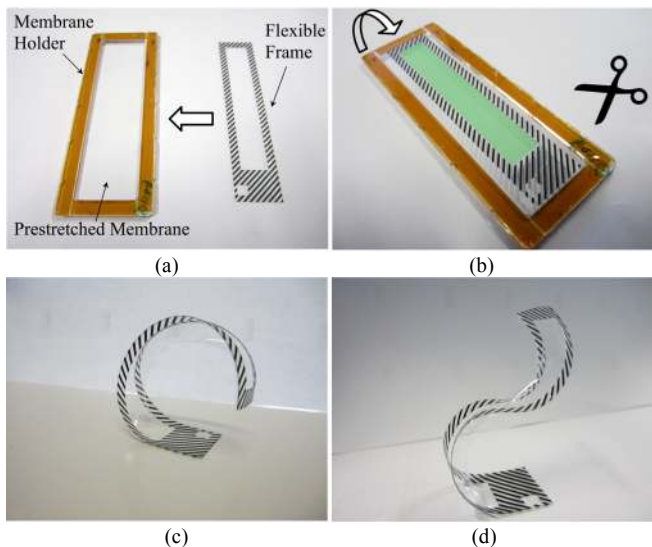
Fig. 2. An example minimum energy structure (MES). (a) On the left, a prestretched polydimethylsiloxane (PDMS) membrane bonded to a rigid plastic holder with Kapton tape and to the right, a flexible but inextensible frame (printed with a hatched pattern on its surface for clarity). (b) The flexible frame bonded to the PDMS membrane surface with a double-sided transparent tape. The frame/membrane structure is released from the plastic holder by cutting the surrounding membrane (in a dielectric elastomer MES actuator, the region shaded in green is covered by a compliant electrode). (c) One minimum energy equilibrium state of the MES. (d) A second equilibrium state.
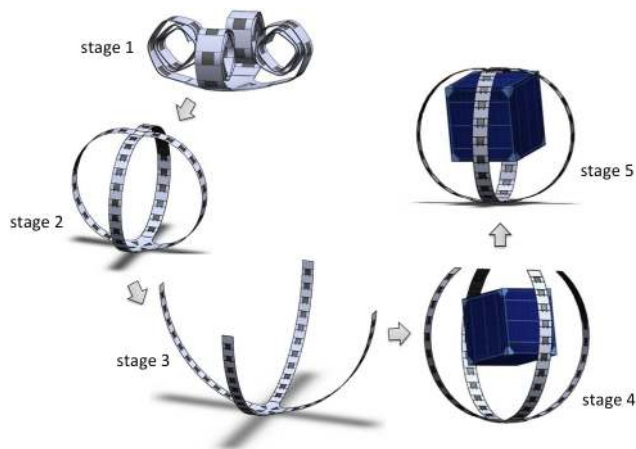

Fig. 3. Schematic of the capture scenario using a DEMES gripper. Stage 1: The DEMES gripper is stored in its rolled state during launch and cruise. Stage 2: The DEMES gripper is deployed and re-assumes its un-actuated form by virtue of the stored elastic forces in DEMES arms. Stage 3: The DEMES gripper is actuated by applying a high voltage, increasing the gripper opening. Stage 4: Once CleanSpace One has rendezvoused with the CubeSat, the DEMES gripper is de-activated. The elastic restorative forces apply a momentum to the capture target causing it to detumble. Stage 5: The DEMES gripper secures the CubeSat with no relative rotation between it and CleanSpace One.

mission serves as an important validation of the concept. A critical aspect of this project is the development of a gripper or end-effector with which to capture the CubeSat. Suggested solutions include capture mechanisms with: a) rigid links (e.g. robotic arms); b) flexible mechanisms (e.g., net, harpoon on a cable); or c) contactless approaches such as ion-beam shepherd [1].

The most suitable capture mechanism depends on many factors, including the debris itself (mass, size, whether it is cooperative or not etc.) and the quality of the information one has on the debris shape and composition. Nets and harpoons can cope with a wide range of debris shapes, and do not require very accurate matching of capture satellite and debris rotations. However nets and harpoons generally only allow for one single attempt at capturing debris (one cannot try again if the first gripping attempt fails) and present a high risk of generating additional debris. Moreover, these devices are essentially passive and so control of their position or shape post-deployment is not possible.

Contactless techniques generate no additional debris, as the target is "pushed" by an ion beam from the capture satellite. The satellite does however require accurate pointing, and must have two ion engines (one to push the debris and another to counter the first), which consume significant electrical power, of order 40W/mN over long time periods. This is incompatible with a small satellite.

Despite the flight heritage of rigid robotic arms, they have important drawbacks for this mission in terms of weight and stowed volume. An interesting approach for the end-effector is the use of dielectric elastomer minimum energy structures

(DEMES) as foldable and compliant gripper mechanisms (Fig. 1(c)). A soft gripper can be used multiple times (on several targets, or repeatedly on the same target if the initial gripping attempt is unsuccessful), and presents only a small risk of generating additional debris.

An example of a minimum energy structure (MES) is shown in Fig. 2. A prestretched elastomer membrane is bonded to an inextensible but flexible frame with an open section. The minimization of the strain and bending energy in the elastomer and frame, respectively, results in complex structures [5]. DEMES, first proposed by Kofod *et al.* [6], take advantage of this energy minimization using voltage-controlled actuation to change the equilibrium state, typically resulting in bending actuation. This is achieved by patterning a compliant electrode on both sides of the elastomer region suspended within the open section (for the MES example shown in Fig. 2, this would be the region shaded in green in Fig. 2(b)). Applying a voltage bias V results in thickness compression due to charge interactions. The resulting compressive pressure produced, often referred to as the Maxwell stress p, is given by,

$$p = e_0 e_r \left(\frac{V}{t}\right)^2. \tag{1}$$

where e_0 is the free space permittivity, e_r is the relative permittivity of the dielectric elastomer and t is the elastomer thickness (the V/t term is the electric field).

The compressive Maxwell stress also gives rise to in-plane prestress relaxation (through material incompressibility [7], [8]), causing a change in equilibrium state and thus actuation [6]. DEMES have shown promise for gripping applications [5], [9] and their inherent flexibility and lightweight nature are
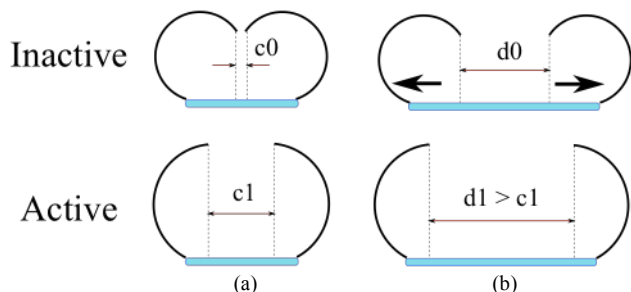
Fig. 4. Schematic cross-section of DEMES gripper (DEMES actuators shown as curved solid black lines, gripper base shown in blue). (a) Actuators placed closed together with a small spacing c_0, resulting in an actuated opening diameter c_1. (b) Actuators spaced further apart with spacing d_0, resulting in a larger actuated opening diameter d_1, relative to c_1.

Fig 5. Actuator design (a) DEMES frame geometries for designs A-C (left to right) (b) DEMES electrode pattern.

advantageous for space applications. Moreover, studies have shown that the material properties of polydimethylsiloxane (PDMS) - an elastomer often used to fabricate DEAs - do not vary substantially over the temperature ranges and radiation levels found in low Earth orbits[1] [10], [11].

Multisegment DEMES differ from single segment versions in that they have more than one open section. This is achieved either by mechanically linking several single segment actuators together [12] or by designing multiple segments into a single frame. For actuators with a high aspect ratio (length versus width) this approach is advantageous as dividing the actuator into multiple segments improves prestretch homogeneity and retention, and restricts the number of stable states the actuator can take (Fig. 2(c)-(d)). Previous attempts at realizing multisegment DEMES involved the use of an acrylic dielectric elastomer and manually applied carbon grease electrodes, both of which are known for their poor long-term performance [12], [13]. Moreover, the manual fabrication approach is a limitation in terms of fabrication accuracy and repeatability.

Here we present a proof of concept multi-segment DEMES actuator for the CSO satellite gripper. Our multisegment actuator uses casted silicone as the dielectric elastomer, and pad printed carbon-silicone composite electrodes for high fabrication accuracy and robustness [14]-[16]. The actuators utilize a single frame with multiple open sections, and are therefore optimized to enable rolled storage prior to deployment. Though developed primarily for CSO, our fundamental DEMES technology and fabrication methods are applicable to other application areas, such as deployable appendages (e.g. legs) for soft mobile robots or manipulators used in manufacturing for grabbing of objects with unknown shapes. In section II we lay out the actuator performance requirements and in section III we present our proof of concept designs and fabrication methodology. Section IV shows the results of the characterization of the actuator designs in terms of bending angle and gripping force. The
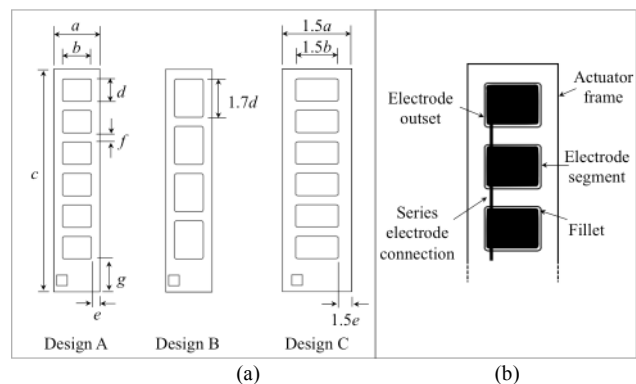
discussion of these results is presented in section V followed the conclusion in section VI.

II. GRIPPER REQUIREMENTS

The proposed CSO microsatellite dimensions are 300 mm × 300 mm × 340 mm (excluding solar panels) and will weigh between 35-40 kg. The gripping target for CSO is the one-unit, 100 mm × 100 mm × 100 mm CubeSat named SwissCube weighing 820g, launched in September 2009, and still operational [16]. SwissCube is smaller than some space debris (which can weigh as much as 9 tons) but many of the technologies required for ADR can be demonstrated at microsatellite scale [1]. The capture of SwissCube presents an important initial goal, laying the foundation for removal of more common scale space debris.

The proposed gripper design uses four multisegment DEMES actuator arms of length 30 cm in a cruciform configuration for secure target gripping. A schematic of the anticipated capture scenario is depicted in Fig. 3. In stage 1, during launch and cruise, the DEMES gripper arms are stored in a rolled configuration to minimize volume. In stage 2, the gripper is released from its rolled configuration and assumes its default state by virtue of its elasticity. In stage 3, the gripper is actuated at high voltage, increasing the size of its opening to accommodate the debris. In stage 4, CSO performs a rendezvous with the CubeSat (by means of onboard debris detection technology [1]) and the voltage to the DEMES gripper arms is switched off. The elastic restorative force in the DEMES actuators causes the gripper to close and come in contact with the CubeSat surface. The DEMES arms exert a moment on the CubeSat causing it to slow its rotational velocity relative to CSO. In stage 5, the gripper secures the CubeSat to CSO, with no relative rotation between CSO and the debris.

A. DEMES Actuator Requirements

We identify two fundamental performance requirements for the DEMES gripper arms: 1) gripping force; 2) bending angle.

---

[1] Temperatures experienced during launch may be outside the range experienced during orbit. However, the gripper will remain stowed during the launch phase and be deployed only once in orbit.
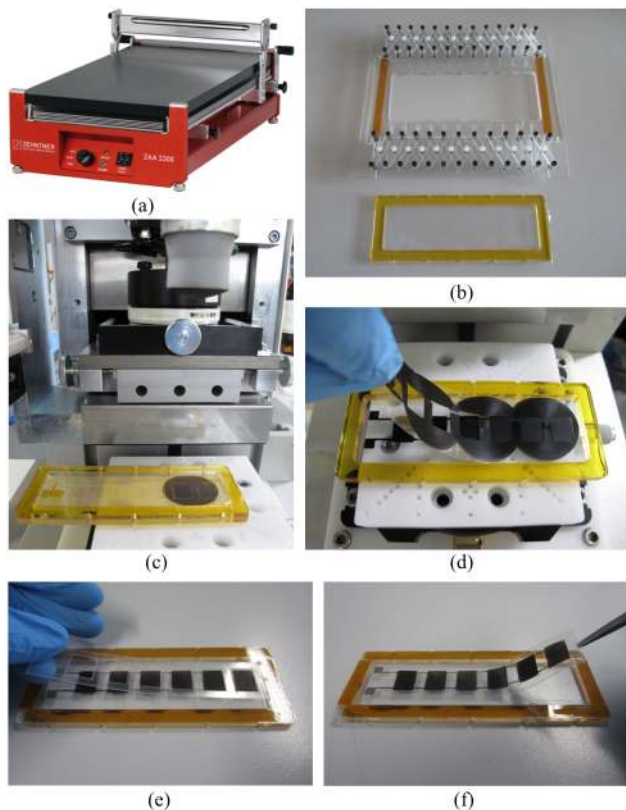
Fig. 6. DEMES actuator fabrication: (a) Zehntner automatic film applicator coater used in the elastomer membrane fabrication (picture source [23]). (b) Pure shear prestretching of membranes using custom built stretcher. (c)-(d) Pad-printing of electrodes through a PET foil mask; (e) Bonding of actuator frame to the elastomer membrane. (f) Releasing of finished actuator.

Gripping force is defined as the reaction force on the DEMES actuator surface (side facing gripping target) arising from the elastic restoring force in the actuator subsequent to the deactivation of the applied voltage (as depicted in stage 4 of Fig. 3). The gripping force required to accomplish this capture scenario was derived in [17] and was found to be between 0.001 mN and 6.5 mN for short detumbling durations (i.e. between 0.5 s and 60 s), and assuming CubeSat initial rotational velocities between 1 and 50 degrees/s.

We describe bending angle in two ways: a) the change of angle of the actuator tip during actuation; and b) the change in projected displacement, which is the difference between c_0 and c_1 (or d_0 and d_1) from Fig. 4, divided by two (see also Fig. 9(b)). The tip angle is a more familiar comparative metric used to characterized bending actuators, where as the projected displacement more directly relates to our gripper application. At the beginning of the detumbling phase the gripper opening needs to be large enough to accommodate the gripping target. This can be guaranteed by appropriately positioning the individual DEMES gripper arms on the gripper base (Fig. 4), such that the size of the gripper opening when the DEMES arms are actuated (c_1 or d_1 from Fig. 4) is larger than the size of the gripping target. However, it should be noted that in future missions, where the capture target is likely
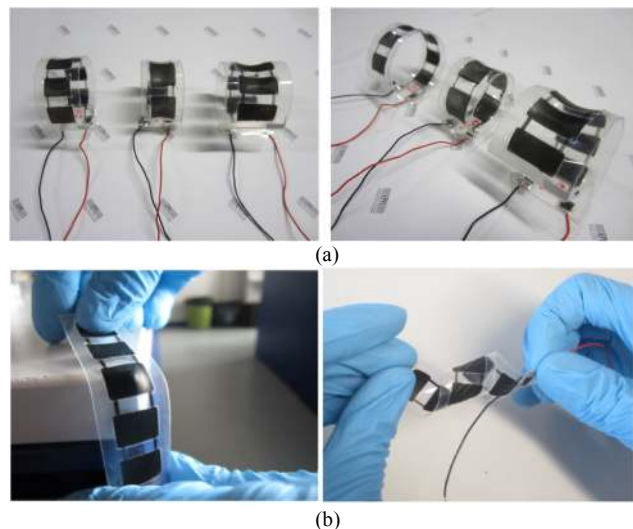

Fig. 7. (a) Fabricated DEMES actuators (un-actuated state), designs A-C from left to right. Each actuator weighs less than 0.65 g. (b) Demonstration of mechanical resilience and robustness of the fabricated DEMES.

to be much larger than the capturing satellite, this may not be a feasible solution. In general, it is desirable that the actuated bending angle be as large as possible for a given actuator geometry to reduce the accuracy required at the rendezvous phase and ensure secure capture.

As an initial step we develop scaled (1:3 in length) versions of the real device to validate the fabrication methodology and prove the concept. These proof of concept devices correspond to a size of actuator that can be conveniently fabricated with our current laboratory set-up. This also enables us to develop and test multiple designs rapidly, acquiring a sense for the important design parameters relating to actuator performance.

III. FABRICATION OF PROOF OF CONCEPT ACTAUTORS

A. Actuator Design

A preliminary investigation into multisegment DEMES [17] guided our prototype actuator designs. We begin with a DEMES design consisting of six segments with a 1:1.3 (length:width) open section aspect ratio (design A). We also characterize two other designs to quantify the effect of varying the number of actuator segments for a fixed actuator length (design B), and the actuator width for a fixed open-section:frame-width ratio (design C). The geometries for these designs, relative to design A, are depicted in Fig. 5 where: $a = 22$ mm, $b = 14$ mm, $c = 105$ mm, $d = 11$ mm, $e = 4$ mm, $f = 4$ mm and $g = 14.5$ mm. For this investigation we consider rectangular shaped segments only to simplify comparisons.

We take the approach of designing multiple segments into a single actuator frame, rather than mechanically linking several independent single segment actuators [12]. This limits the chance of over-stiffening the actuator (thus inhibiting rolled storage) and simplifies fabrication.

Fig. 8. Fabricated DEMES actuators wrapped around objects of various shapes and sizes to demonstrate conformability. Objects are (from left to right, top to bottom): Toblerone bar, PMMA piece laser cut into the shape of a fictional spacecraft, an apple, a model of SwissCube.
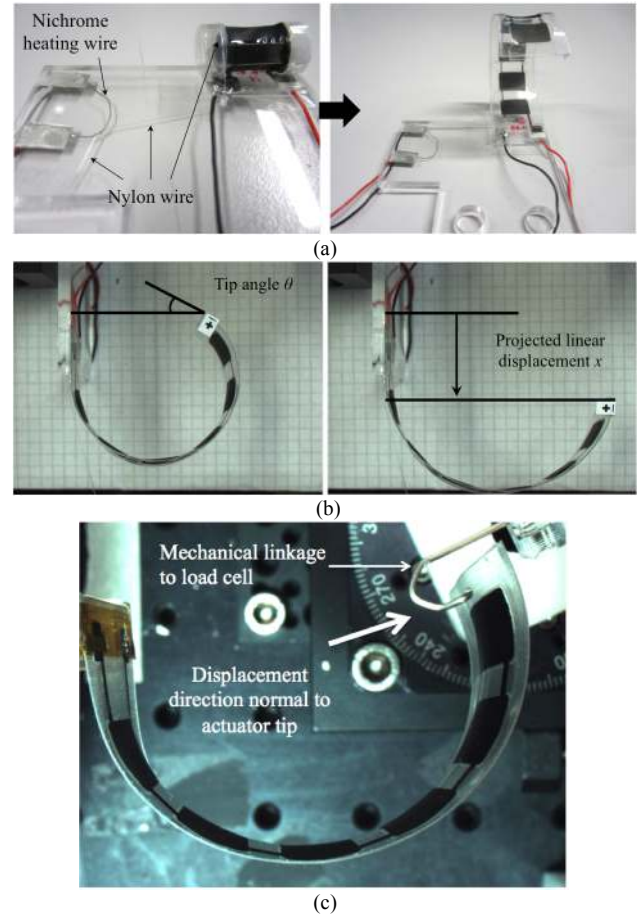

Fig. 9. (a) Actuator release mechanism; left while rolled-up, right, after releasing by melting the nylon wire. (b) Actuator design A at 0 V (Left) and 3800 V (Right) All measurements were done in air and at room temperature. Tip angle and projected displacement indicated; (c) Gripping force measurement set-up. Metal mechanical linkage connected to a load cell measures reaction force near the actuator tip as the load cell is linearly displaced away from the actuator.

The segment electrode geometry was inset by 500 μm relative to the flexible frame geometry to prevent failure by over constraining the actuation zone. The corners of the electrodes were also filleted to prevent localized electric field concentrations, which could lead to premature actuator failure. We drive all the actuator segments simultaneously, thus tracks are incorporated into the electrode design that connect all the electrode segments electrically in series, and terminate at the base of the actuators. If required (for independent segment actuation for example), parallel electrical connection of the segments can be achieved simply by changing the electrode mask pattern (see section III.C).

In future designs, sensing could be incorporated directly into the electrode design by means of dielectric elastomer switches [18], or by "self-sensing" of the electrode capacitance [19]. This would increase the device functionality providing feedback on the state of the actuator (i.e. deployed, non-deployed, successful target capture etc.). Alternatively, printed flexible electronics techniques could be utilized to embed sensing capabilities directly into the actuator frame [20].

Following the work of Kofod et al. [5] we use initially a pure shear stretch state in prestretching our elastomer membranes i.e. stretching in one planar dimension whilst keeping the other constant. Work has been done in trying to characterize the effect of elastomer membrane prestretch on performance for single segment devices [14], [21], [22], but similar analyses for multisegment devices are yet to be performed.

B. Elastomer membrane preparation

We used a two-part silicone elastomer (Sylgard 186, Dow Corning) as the dielectric elastomer. The base and curing agent were mixed at a 10:1 ratio respectively, using a planetary mixer (Thinky ARE-310). The mixture was further thinned using a silicone solvent (OS-20, Dow corning) and blade cast onto a plastic substrate to a thickness of approximately 70 μm using a Zehntner automatic film applicator coater (Fig. 6(a)). The membrane was subsequently cured in an oven at 80°C degrees for approximately one hour.

The cured elastomer membrane was cut into 80 mm long by 45 mm wide sections and peeled from the substrate. The elastomer was then adhered to two rigid holders and pre-stretched in pure shear to 1.3 times its original length using a purpose built prestretch device (Fig 6(b)). The film was then affixed to a rigid plastic holder lined with double-sided Kapton tape to maintain its prestretch.

C. Electrode Realization

Compliant electrodes are a key challenge for DEAs [13]. Our electrodes are realized via a stamping method using a Teca Print TPM101 pad-printing machine. The machine operates by doctor blading a small amount of liquid electrode material onto a shallow reservoir, which is subsequently picked up by a rubber stamp. The stamp then applies the ink onto the elastomer membrane surface through a PET foil mask which is laser cut with the desired electrode pattern. This
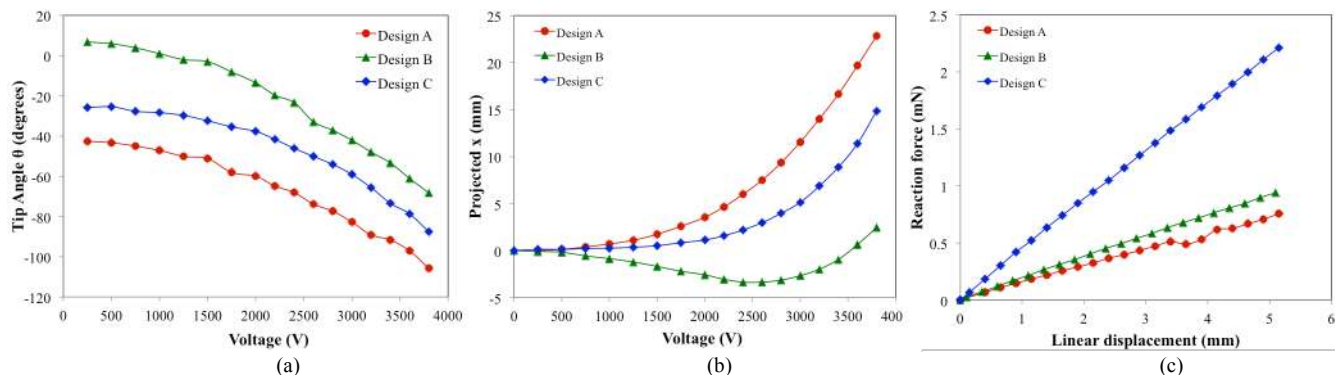
Fig. 10. Results of actuator characterization for a range of input voltages. (a) Actuator tip angle. (b) Projected linear displacement of actuator tip. (c) Gripping force.

enables creation of accurate and repeatable electrodes. The electrode is then cured in an oven at 80°C and the process is repeated on the reverse side of the elastomer membrane.

The ink used is composed of carbon black in a silicone elastomer matrix. The silicone used in the electrode ink is the same used to make the dielectric elastomer membrane, this helped ensure adequate bonding. The resulting electrodes were measured to be approximately 2 micrometers thick. The cured electrodes are robust providing improved longevity and resilience to mechanical deformation (Fig 7(b)) compared to methods using grease-based electrodes [12], [21].

D. Adhering of actuator frame

The actuator frame was made by laser cutting a 100 μm thick transparent polyester foil (typically used in inkjet printing) with a 50 μm thick transparent silicone adhesive layer (ARClear 8932, Adhesives Research) adhered to its surface. The laser cut frame-adhesive was bonded to the elastomer membrane (Fig. 6(e)) and was manually aligned with the pad-printed electrodes. The actuator was subsequently released using scissors (Fig 6(f)).

The resulting actuators (Fig. 7(a)) are light, weighing no more than 0.65 g (excluding electrical connections), demonstrating a high degree of flexibility and mechanical resilience (Fig. 7(b)), and conformability to objects of various shapes and sizes (Fig. 8).

IV. ACTUATOR CHARACTERIZATION

A. Measurement set-up

The actuators were rolled up (about the width axis) manually into a cylinder of outer diameter between 12 and 14 mm prior to commencing the bending and gripping force experiments to simulate storage on the satellite. The actuators were then released using a deployment mechanism similar to that used on SwissCube to deploy its antenna. The rolled actuators were secured using nylon wire, which is passed along a nichrome heating wire as shown in Fig. 9(a) (0.8 gauge, RS components). The actuators were subsequently deployed by applying a current of 1.89 A (duration no more than 2 seconds) through the nichrome wire, melting the nylon wire and allowing the actuators to unfurl naturally as a result

of the stored elastic energy. The actuators were allowed to stabilize prior to measurements being taken.

For the bending angle measurements the actuators were placed on their side to minimize gravity effects. Incremental voltage steps were supplied to the actuator at 250 V intervals in the range 0 – 2 kV, and at 200 V intervals in the range 2 – 3.8 kV, minimizing dynamic effects. The input voltages were supplied by an Auckland Biomimetics Lab EAP high voltage power supply. Still images were taken at each voltage step using a CMOS camera (Point Grey FMVU-13S2C) a few seconds after application of the voltage increment to allow the actuators to reach steady state. The images were subsequently post processed in software (ImageJ, National Institutes of Health). The tip angle θ and the projected linear displacement x of the actuator tip are defined in Fig. 9(b). Tip angles are taken relative to the horizontal line shown in Fig. 9(b) left, with clockwise angle rotations denoting negative tip angles.

For the gripping force measurements, a load cell (FUTEK LRF400) was used to measure the reaction force on the actuator as a function of an imposed linear displacement (Fig. 9(c)). All measurements were conducted at the actuator tip and displacements made normal to the actuator surface. As a simplification we assume securement of the capture target occurs in a position close to the DEMES initial (un-actuated) position, hence we record the forces at small deflections from this initial position (approximately 5 mm linear displacement).

B. Experimental results

After unrolling the actuators a small change in the initial position was observed compared to the state before rolling-up, which we attribute to creep in the actuator frame material. This was less noticeable in the actuator design C, which had an overall stiffer frame.

Fig. 10(a) shows that all the actuators displayed a quadratic relationship between tip angle and actuated voltage, a behavior in agreement with previously reported experiments for single segment devices [14], [21]. Actuator design A showed the largest initial tip angle (comparatively low actuator curvature) and final angle at -43 degrees and -106 degrees, respectively. Conversely actuator design B showed the lowest initial tip angle (comparatively high curvature) and final angle. All

actuator designs experienced a similar change in tip angle of between 61 - 63 degrees in the range of the applied voltage.

Actuator design A also showed the largest projected linear displacement of approximately 22 mm (Fig. 10(b)), with design C showing the second largest displacement of approximately 15 mm. Actuator design B displayed a non-quadratic, non-monotonic response on voltage: first displaying negative displacements (relative to convention showed in Fig. 9(b).), finding a minimum at approximately -3.3 mm before experiencing positive displacements with a maximum of approximately 2.4 mm. This behavior is due to the initially high curvature of the actuator.

The results of the gripping force measurements are shown in Fig 10(c). Force measurements were taken up to a linear displacement of approximately 5 mm (5% of the length of the actuators when flat) for all measurements. All the actuator designs displayed an approximately linear response on actuator tip displacement. Actuator design C showed the largest force at maximum displacement of 2.2 mN. Actuator designs A and B showed similar force values with design B having a larger maximum force of 0.94 mN, compared to the 0.76 mN of actuator design A.

V. DISCUSSION

Single frame multisegment DEMES actuators utilizing silicone elastomers have been developed. The materials used were inexpensive and the resulting actuators exhibit a high degree of conformability and mechanical resilience. Use of non-grease-based, pad-printed composite electrodes and low creep silicone help ensure longevity and repeatability of operation. As a result of these features, the actuators showed successful operation even after being rolled into cylinders of diameter less than one seventh of the actuator flat length, proving the proposed stowage concept. To the best of the authors' knowledge this is the first gripper with this capability developed for space applications. Additionally, the actuators were deployed using a mechanism similar to that used in previous satellite missions. This ability for rolled storage and deployment becomes increasingly important for future missions and as the size of capture targets increases beyond that of SwissCube.

The actuators showed some creep behavior whilst in the rolled state[2], frames made from low creep materials such as polyethersulfone (PES) could be employed in future designs to mitigate this effect. Moreover, frames made from casted silicone elastomers or elastomer composites [24] could also be used. However, these could result in increased mass and limit the minimal rolling diameter. It should be noted that although we primarily consider rolled storage here, other low volume storage configurations, e.g. laying flat against the exterior of the satellite, are possible with our multisegment DEMES actuators.

Only a single equilibrium state was observed with the

actuators due to the multisegment approach. This is an essential feature as an actuator capable of snapping between equilibrium states would be undesirable for our gripping application.

The results of the bending angle measurements show that the three actuator designs display approximately the same change in tip angle for a given applied voltage despite their differing designs. This is somewhat intuitive as the actuator lengths are the same in each case, as is the approximate total volume of elastomer material suspended in the open sections. However, it is unclear how the bending energy correlates with the tip angle i.e. whether the change in tip angle is independent of the initial angle, for a given electric field input. Hence, the observed trends could be a mixture of electromechanical and geometric effects.

The initial tip angle correlates with the segment aspect ratio i.e. the designs having a high segment aspect ratio (length to width) also having the lowest initial tip angle (highest curvature). This could be the result of bending about the length axis of the actuators. Actuators with low segment aspect ratios would experience more bending about the length axis, resulting in an increase in the stiffness of the frame about the width axis. A similar effect has also been observed in finite element simulations of single segment DEMES with high width prestretch [21]. In our work pure shear prestretched membranes were used exclusively, however other prestretch states may yield greater changes in angle for a given applied electric field, or the same change for a lower input voltage [15], [25].

The results of the projected displacement show that though the actuators experience a similar change in tip angle with applied voltage, actuator design A, with the largest segment aspect ratio, showed the largest projected displacement. This result is most likely dominated by the actuator initial curvature as all the actuators displayed similar total tip angle change, but the designs with the largest initial tip angle (smallest curvature) experienced a larger projected displacement.

The results of the gripping force measurements showed that actuator design C, which had the largest total width, had also a substantially larger (more than double) force than the other designs. This is an important design conclusion indicating that, for a given actuator length, greater force can be achieved simply by increasing the width of the segment and frame geometry proportionally, whilst retaining the same change in tip angle, for a given input voltage. This will be particularly important when the actuator is scaled up to its full 30 cm length, where the gripping force is expected to decrease. Moreover, multiple dielectric elastomer layers could be used, in combination with proportionally thicker actuator frames, and should yield similar performance in terms of change in tip angle, whilst increasing gripping force. The increase in force with linear displacement is an advantageous feature, providing a positive mechanical feedback loop, with the reaction force increasing if the gripping target begins to move away during capture.

---

[2] Though once deployed no change in the shape of the actuators was observed during a storage period of several months.

VI. CONCLUSION

We have presented proof of concept, multisegment dielectric elastomer minimum energy structure (DEMES) actuators as the fundamental component of a deployable microsatellite gripper. The actuators possess uniquely advantageous properties for this application including their low mass, damage resilience and mechanical flexibility, enabling rolled storage prior to deployment and successful operation. These devices can currently be made at relative low cost whilst maintaining good repeatability, accuracy and mechanical resilience. Three small-scale actuator designs were fabricated and characterized in terms of bending angle, for an applied voltage, and gripping (reaction) force. All the actuators were rolled prior to deployment and testing. Our devices, weighing less than 0.65g, produced a change in tip angle of approximately 60 degrees, and a maximum gripping force of 2.2 mN for small displacements of the actuator tip. This initial investigation has proved the concept of using rolled multisegment DEMES for volume efficient gripper storage, and provided a road map for future actuator development.

ACKNOWLEDGMENT

REFERENCES

[1] M. Richard, L. Kronig, F. Belloni, S. Rossi, V. Gass, S. Araomi, I. Gavrilovich, H. Shea, C. Paccolat, J.P. Thiran, "Uncooperative Rendezvous and Docking for MicroSats, The case for CleanSpace One", Presented at the 6th International Conference on Recent Advances in Space Technologies, RAST 2013, 12-14 June 2013, Istanbul, Turkey.
[2] Swiss Space Centre, "SWISSCUBE." [Online]. Available: http://swisscube.epfl.ch/. [Accessed: 24-Sep-2013].
[3] J. –C. Liou, "An active debris removal parametric study for LEO environment remediation. *Advances in Space Research*. Vol. 14, pp. 1865-1876, Feb. 2011.
[4] Swiss Space Centre, "Clean-mE Project," 2012. [Online]. Available: http://space.epfl.ch/page-61745-en.html. [Accessed: 23-Sep-2013].
[5] G. Kofod, W. Wirges, M. Paajanen, and S. Bauer, "Energy minimization for self-organized structure formation and actuation," *Applied Physics Letters*, vol. 90, no. 8, p. 081916, 2007.
[6] G. Kofod, M. Paajanen, and S. Bauer, "Self-organized minimum-energy structures for dielectric elastomer actuators," *Applied Physics A*, vol. 85, no. 2, pp. 141–143, Sep. 2006.
[7] R. Pelrine, R. Kornbluh, and Q. Pei, "High-speed electrically actuated elastomers with strain greater than 100%," *Science*, vol. 287, no. 5454, pp. 836–839, Feb. 2000.
[8] Z. Suo, "Theory of dielectric elastomers," *Acta Mechanica Solida Sinica*, vol. 23, no. 6, pp. 549–578, 2010.
[9] I. A. Anderson, T. a. Gisby, T. G. McKay, B. M. O'Brien, and E. P. Calius, "Multi-functional dielectric elastomer artificial muscles for soft and smart machines," *Journal of Applied Physics*, vol. 112, no. 4, p. 041101, 2012.
[10] M. Niklaus, S. Rosset, and H. Shea, "Array of lenses with individually tunable focal-length based on transparent ion-implanted EAPs," in *Proc. SPIE*, 2010, vol. 7642, p. 76422K–76422K–12.
[11] J. C. Lötters, W. Olthuis, P. H. Veltink, and P. Bergveld, "The mechanical properties of the rubber elastic polymer polydimethylsiloxane for sensor applications," *J. Micromechanics Microengineering*, vol. 7, no. 3, p. 145, 1997.
[12] M. T. Petralia and R. J. Wood, "Fabrication and analysis of dielectric-elastomer minimum-energy structures for highly-deformable soft robotic systems," *2010 IEEE/RSJ International Conference on Intelligent Robots and Systems*, pp. 2357–2363, Oct. 2010.
[13] S. Rosset and H. R. Shea, "Flexible and stretchable electrodes for dielectric elastomer actuators," *Applied Physics A*, pp. 281–307, Nov. 2012.
[14] J. Shintake, S. Rosset, D. Floreano, and H. R. Shea, "Effect of mechanical parameters on dielectric elastomer minimum energy structures," in *Proc. SPIE*, 2013, vol. 8687, p. 86872V–86872V–13.
[15] S. Akbari, S. Rosset, and H. R. Shea, "Improved electromechanical behavior in castable dielectric elastomer actuators," *Applied Physics Letters*, vol. 102, no. 7, p. 071906, 2013.
[16] L. Maffli, S. Rosset, and H. R. Shea, "Zipping dielectric elastomer actuators: characterization, design and modeling," *Smart Materials and Structures*, vol. 22, no. 10, p. 104013, Oct. 2013.
[17] I. Gavrilovich, "Study of a Dielectric Elastomer Gripper for Cleanspace One," 2013. [Online]. Available: http://infoscience.epfl.ch/record/188245?ln=en
[18] B. M. O'Brien, E. P. Calius, T. Inamura, S. Q. Xie, and I. A. Anderson, "Dielectric elastomer switches for smart artificial muscles," *Appl. Phys. A*, vol. 100, no. 2, pp. 385–389, Jun. 2010.
[19] T. A. Gisby, B. M. O'Brien, and I. A. Anderson, "Self sensing feedback for dielectric elastomer actuators," *Appl. Phys. Lett.*, vol. 102, no. 19, p. 193703, 2013.
[20] H. Al-Chami and E. Cretu, "Inkjet printing of microsensors," in *2009 IEEE 15th International Mixed-Signals, Sensors, and Systems Test Workshop*, 2009, pp. 1–6.
[21] B. O'Brien, T. McKay, E. Calius, S. Xie, and I. Anderson, "Finite element modelling of dielectric elastomer minimum energy structures," *Applied Physics A*, vol. 94, no. 3, pp. 507–514, Nov. 2009.
[22] S. Rosset, O. Araromi, H. R. Shea, "Model and design of dielectric elastomer minimum energy structure", under review.
[23] Zehntner Testing Instruments, [Online]. Available: http://www.zehntner.com.
[24] W. Shan, T. Lu, and C. Majidi, "Soft-matter composites with electrically tunable elastic rigidity," *Smart Materials and Structures*, vol. 22, no. 8, p. 085005, Aug. 2013.
[25] T. Lu, J. Huang, C. Jordi, G. Kovacs, R. Huang, D. R. Clarke, and Z. Suo, "Dielectric elastomer actuators under equal-biaxial forces, uniaxial forces, and uniaxial constraint of stiff fibers," *Soft Matter*, vol. 8, no. 22, p. 6167, 2012.

Oluwaseun Araromi received his undergraduate education in Mechanical Engineering at the University of Bristol and the University of Illinois at Urbana-Champaign, and received his M.Eng. degree in 2008 from the University of Bristol. He continued his studies at the University of Bristol, commencing his doctoral work in electroactive polymer actuators. He received his Ph.D. degree in 2012.

From May to June 2007 he worked as a Research Assistant in the Mechanical Engineering department at the University of Illinois at Urbana-Champaign. He currently holds a postdoctoral position at the Microsystems for Space Technologies Laboratory, École Polytechnique Fédérale de Lausanne (EPFL). His research pursuits include the development and optimization of dielectric elastomer actuators for reconfigurable antenna and flexible grippers.

Dr. Araromi was the recipient of a University of Bristol Scholarship which funded his Ph.D. degree.

Irina Gavrilovich was born in Yasnogorsk, Tula Region, Russia, in 1989. She obtained her M.Eng. degree (with honor) in aerospace engineering from Bauman Moscow State Technical University (BMSTU), Russia, in 2012. She is currently pursuing a Ph.D. degree at Université Montpellier 2, Montpellier Laboratory of Informatics, Robotics and Microelectronics, France.

From 2009 to 2012, she was part-time Engineer in Prospective Space Technologies Laboratory of BMSTU Youth Space Center. From 2011 to 2012,

she was part-time Engineer in Research and Production Enterprise VNIIEM. From 2012 to 2013, she was researcher at École Polytechnique Fédérale de Lausanne (EPFL), Microsystems for Space Technologies Laboratory and Swiss Space Center.

Ms. Gavrilovich's awards include Scholarship of Academic Senate (BMSTU), Scholarship of Imperial Technical School (BMSTU) and Swiss Government Scholarship.

Samuel Rosset received the M.S. (2004) and Ph.D. (2009) degrees in microengineering from the école polytechnique fédérale de Lausanne (EPFL), Switzerland.

From 2005 to 2008, he was a research assistant with the microsystems for space technologies laboratory (LMTS) at EPFL, Switzerland. After a few years in industry developing tuneable optics based on soft elastomers, he re-integrated the LMTS in 2011 where he is now working as a research scientist, overseeing the activities on dielectric elastomer actuators. His research interest includes soft actuators, compliant electrodes and the development of new fabrication processes for soft sensors and actuators. His research focuses on reliability and lifetime of these devices.

Jun Shintake received his B.Eng. degree and M.Eng. degree in Mechanical Engineering from the University of Electro-Communications, Tokyo, Japan, in 2009 and 2011, respectively.

Currently he is a PhD student at the Laboratory of Intelligent Systems and the Microsystems for Space Technologies Laboratory, École Polytechnique Fédérale de Lausanne (EPFL), Lausanne, Switzerland. His research interest includes smart materials, intelligent structures, and their use in the field of robotics especially soft, bio-inspired, reconfigurable, foldable, and aerial robotics.

Muriel Richard, Mrs. Richard holds a M.Sc. degree (1996) in Mechanical Engineering from the California Institute of Technology. She worked at the NASA's Jet Propulsion Laboratory from 1994 till 2005, early on for the Mars Program, and then for the Advanced Propulsion Technology Group.

She became a senior engineer in 2001 when she moved to JPL's Mission Architecture Group. In 2005, she was employed by the Space Center EPFL in Switzerland to manage the SwissCube satellite project, and later managed the "Clean-mE" research and technology development program on Active Debris Removal. Since January 2012, she is the Deputy Director of the newly renamed Swiss Space Center.

Volker Gass, photograph and biography not available at the time of submission.

H. R. Shea (SM'2009) holds a B.Sc. degree (1991) in physics from McGill University, and a Ph.D. degree (1997) in physics from Harvard University. He developed carbon nanotube FETs at IBM's T.J. Watson Research Center from 1997 to 1999, then joined Lucent Technologies' Bell Labs in Murray Hill, NJ, where he became the technical manager of the Microsystems Technology group, specializing in MEMS reliability. In 2004 he founded the Microsystems for Space Technologies Laboratory at the EPFL (École Polytechnique Fédérale de Lausanne) in Switzerland, where he is an associate professor since 2011. Current research topics include micromachined soft polymer actuators and sensors, MEMS ion sources for micro-propulsion of small spacecraft, and MEMS reliability.